

Hydrodynamic Interactions in Flow Past Grafted Polymers

V. Kumaran

*Department of Chemical and Nuclear Engineering, University of California, Santa Barbara, California 93106**Received September 24, 1992; Revised Manuscript Received February 8, 1993*

ABSTRACT: The effect of hydrodynamic interactions in a grafted polymer brush under shear flow is examined. It is shown that the hydrodynamic interactions in a strained brush cause an increase in the brush thickness due to an asymmetry in the pair distribution of monomers. The predictions are in qualitative agreement with some recent experiments.

I. Introduction

The equilibrium properties and phase transitions of polymer "brushes" have been widely studied.¹ A brush consists of polymer molecules end-grafted onto a solid surface such that the distance between the points of attachment, d , is small compared to the radius of gyration of a single polymer molecule in a solvent or a melt. Due to the proximity of the grafting points, the polymers are highly stretched and the thickness of the brush is large compared to the radius of gyration of a polymer in solution. This thickness is determined by a balance between the elastic tension along the chain and the osmotic pressure due to the excluded-volume interactions between the monomers. Alexander and de Gennes^{2,3} used scaling arguments to show that the brush thickness varies as $Nd^{-2/3}$; this scaling law has been subsequently verified by more detailed theoretical calculations⁴ and experiments.⁵ Thus, the brush thickness is proportional to the number of monomers N , in contrast to the $N^{1/2}$ and $N^{3/5}$ dependencies of the radius of gyration of a polymer in a melt and a solvent, respectively.

Rabin and Alexander⁶ were the first to study the effect of a shear flow at the surface of a polymer brush. They treated the brush as a collection of closely packed concentration blobs, each having a diameter equal to the distance between grafting points. The effect of the shear flow was approximated by a force acting at the free surface of the brush. This force causes an elongation and tilt of the polymers in the direction of the flow, but the theory predicts that the thickness of the layer is unaltered by the force at the surface. However, experimental studies by Klein et al.⁷ using a surface force measurement apparatus showed that there is an increase of up to 20% in the brush thickness due to a shear flow. Barrat⁸ subsequently revisited the Rabin and Alexander calculation and showed that the theory is capable of predicting an increase in the brush thickness. This is caused by a decrease in the osmotic compressibility due to the force acting at the free surface.

In this paper, we analyze the effect of hydrodynamic interactions in a polymer brush when a shear flow is applied at the surface. We find that the interactions cause a net upward force on the polymers, which could lead to an increase in the brush thickness. The change in the brush thickness is calculated as a function of the shear velocity, and the theoretical predictions are compared with the experimentally observed increase in the brush thickness.

II. Theory

At the outset, it is useful to get an idea of the numerical values of the parameters that could influence the dynamics of the brush. The height, L , of the polymer brush used

by Klein et al.⁷ was about 750 Å, and the radius of gyration, R_G , of the polymers in a good solvent was reported to be 320 Å by Tounton et al.⁵ On the basis of these values, Barrat⁸ estimated that the grafting distance between the polymers was about 75 Å. The brushes were sheared past each other at a frequency of 200–400 s⁻¹ and at velocities of about 1–2 mm/s in the experiments. The time required for the fluid velocity profile to respond to changes in the boundary velocities scales as L^2/ν , where ν is the kinematic viscosity of the fluid. For normal fluids, ν is about 10⁻⁶ m²/s, and the fluid response time is 10⁻⁸ s. This is small compared to the strain rate in the fluid and the frequency of oscillation of the surfaces, and therefore we can neglect the fluid inertia in the analysis. The longest Rouse time for the polymer, which is the response time of the polymer to changes in the fluid flow, is $\eta R_G^3/k_B T$ (Doi and Edwards,¹⁰ Chapter 4), which is 0.27×10^{-5} s for the parameters listed above. This is small compared to the period of oscillation of the surfaces in the experiments, which were about 0.2×10^{-2} s, and in the analysis we assume that the brush configuration responds instantaneously to the changes in the velocity of the surfaces. This approximation is supported by the experimental results of Klein et al.,⁷ who found that the swelling is only a function of the velocity of the surfaces and not the frequency of oscillation; variations in the frequency between 200 and 500 s⁻¹ did not alter the brush thickness appreciably.

The height of a brush scales as $Nb(b/d)^{2/3}$ in a good solvent and $Nb(b/d)$ in a Θ solvent. This is much larger than the radius of gyration of a single polymer in a good solvent, which scales as $N^{3/5}b$, and the polymers are highly stretched in the direction perpendicular to the grafting surface. The average positions can be thought of as lying along a "classical trajectory" in this direction, and the monomer positions fluctuate about this classical trajectory by a distance of order d . There is one other length scale, the screening length for hydrodynamic interactions, which plays an important role in our analysis. The velocity disturbance due to an isolated particle moving in a fluid decreases as $1/r$ where r is the distance from the particle. In a polymer solution, however, the disturbance decays exponentially at distances greater than the screening length ξ_H due to the flow caused by the surrounding monomers. This screening length, ξ_H , is $2/(\pi cb^2)$, where c is the concentration of monomers and b is the segment length.¹⁰ In a good solvent, the screening length is $O(d/b)^{1/3}$ larger than the spacing between the grafting points, d , but is $O(d^2/Nb^2)$ smaller than the height of the brush. In this paper, the hydrodynamic interactions are analyzed in the asymptotic limit $d \ll \xi_H \ll L$. This assumption will not give us numerically accurate results for the brushes used by Klein et al.⁷ because the grafting distance d is smaller

than the height of the brush only by a factor of about 10, and this does not leave adequate room for an intermediate scale. However, these assumptions should give us accurate scaling relations and order of magnitude estimates.

In a Θ solvent the screening length is of the same magnitude as the grafting distance, d . As a result, the hydrodynamic interactions are screened over a very short distance and would not increase the height of the brush appreciably. Interestingly, the same conclusion was reached by Barrat,⁸ who considered a completely different mechanism for the brush expansion. This distinction between good solvents and Θ solvents could be used to test the validity of the theories.

The analysis is carried out in two steps. First, we calculate the change in the polymer conformations due to the shear flow in the absence of hydrodynamic interactions. This leading order calculation shows that the polymers are stretched along the flow direction, and there is no increase in the height of the brush. The straining of the polymers causes an asymmetry in the pair distribution function of the monomers and tends to cause a net flow in the direction perpendicular to the grafting surface. However, a net flow in this direction is not permitted by the continuity equation, and to suppress this flow, there is a force exerted on the monomers which tends to expand the brush. In the second step, we calculate the net force required to suppress the flow perpendicular to the grafting surface and the expansion of the brush.

The brush is modeled as a close-packed array of blobs of size d , each of which has $(d/b)^{5/3}$ monomers. In the classic Alexander-de Gennes^{2,3} picture, the concentration profile is a step function and all the free ends of the polymers are at the free surface. However, more detailed calculations by Milner, Witten, and Cates⁴ show that the concentration profile is parabolic and decreases from a maximum at the grafting surface to zero at the free surface.

$$\phi(y) = \phi_0(y^2/L^2) \quad (2.1)$$

where $\phi(y)$ is the volume fraction of monomers at position y and ϕ_0 is the concentration at the grafting surface.

When a shear flow is applied at the surface of the brush, the velocity is a decreasing function of y due to the frictional force exerted by the monomers. It was shown by Milner⁹ that the hydrodynamic penetration depth, which is the depth to which the fluid velocity penetrates into the brush, is sensitive to the concentration profile of the monomers. For a step profile the penetration depth scales as ξ , the mesh size, whereas for a brush with a parabolic concentration profile the fluid velocity penetrates to a much greater depth of $O(\xi L)^{1/2}$, which is the geometric mean of the mesh size and the height of the brush. Milner⁹ calculated the leading order velocity profile, $v_{x0}(y)$, using the Brinkman equation¹¹ and neglecting hydrodynamic interactions between the monomers. For a one-dimensional flow along the x axis, the Brinkman equation reduces to

$$\eta \frac{\partial^2 v_{x0}}{\partial y^2} - \frac{\eta}{\xi^2} v_{x0} = 0 \quad (2.2)$$

where η is the fluid viscosity and ξ is the mesh size which depends on the local concentration of monomers. While calculating the velocity profile, Milner⁹ assumed that the penetration depth is large compared to the mesh size at the grafting surface, ξ_0 , but small compared to the height of the brush, L .

Table I. Scalings of the Parameters That Influence the Brush Dynamics and Their Numerical Values in the Experiments of Klein et al.⁷

parameter	scaling relation	exptl value
no. of monomers	N	
vol fraction of monomers	ϕ	0.1
segment length	b	
grafting distance (Å)	d	75
radius of gyration (Å)	R_G	320
brush height (Å)	$L \sim Nb(b/d)^{2/3}$	750
hydrodynamic screening length (Å)	$\xi_H \sim (1/cb^2)$	250
fluid density (kg/m ³)	ρ_f	10 ³
polymer density (kg/m ³)	ρ_p	10 ³
fluid kinematic viscosity (m ² /s)	ν	10 ⁻⁶
brush modulus (kg/m/s)	$k_B T/\xi^3$	10 ⁴
fluid velocity (mm/s)	v_{x0}	1-2
frequency (s ⁻¹)	ω	200-500
fluid response time (s)	L^2/ν	10 ⁻⁸
polymer response time (s)	$0.325\eta R_G^3/k_B T$	0.27×10^{-5}

The frictional force, f_x , exerted on a monomer by the fluid flow, is given by

$$f_x = (6\pi\eta b_H)v_{x0}(y) \quad (2.3)$$

where b_H is the hydrodynamic radius of the monomers and is of the same magnitude as the segment length b . This force causes a displacement of the monomers in the x direction, which can be calculated from a steady-state force balance equation for a segment between monomers n and $n+1$:

$$f_x|_{n+1} - f_x|_n = k(x_{n+1} - x_n) \quad (2.4)$$

In the above equation, the spring constant, k , is $3k_B T/b^2$. In the limit of large N , the monomer positions can be expressed as continuous functions of the index n and the force balance equation assumes the following form:

$$\frac{\partial f_x}{\partial y} = k \left(\frac{\partial x_n}{\partial n} \right) / \left(\frac{\partial y_n}{\partial n} \right) \quad (2.5)$$

The right side of the above equation is the product of the spring constant and the local slope of the classical trajectory. Though the force exerted by the fluid causes a displacement of monomers in the x direction, it does not affect the density profile and the osmotic pressure gradient due to excluded-volume interactions in the y direction. Therefore, the brush height remains unchanged in the leading approximation.

The slope of the classical trajectory plays an important role in the analysis, and it is useful to determine its dependence on the brush parameters. The drag force on one correlation blob scales as $6\pi\eta v_{x0}d$, and its spring constant scales as $3k_B T/d^2$. The displacement in the x direction across one blob is the ratio of the force and the spring constant, and the slope of the classical trajectory is the ratio of the displacement and the diameter of the blob, d :

$$\tan(\theta_0) = 2\pi\eta v_{x0}d^2/k_B T \quad (2.6)$$

For small v_{x0} , the angle of inclination θ_0 increases proportionally to $2\pi\eta v_{x0}d^2/k_B T$, whereas in the limit of large v_{x0} , θ_0 is proportional to $\pi/2 - k_B T/2\pi\eta v_{x0}d^2$. For the values of d , η , and v_{x0} listed in Table I, the slope of the classical trajectory, $\tan(\theta_0)$, varies between 0.1 and 1.

The force exerted by the monomers on the fluid causes a correction to the leading order flow due to hydrodynamic interactions. We calculate this additional velocity using the point particle approximation, in which the monomers are considered to be point forces in the fluid. The velocity disturbance at the origin, $\mathbf{v}_1(0)$, caused by a point force

$f_0(\mathbf{r})$ at point \mathbf{r} , is given by the Oseen tensor:

$$v_{i1}(0) = \frac{-1}{8\pi\eta r} \left(\delta_{ij} + \frac{r_i r_j}{r^2} \right) f_{j0}(\mathbf{r}) \quad (2.7)$$

where we have used the Einstein notation to represent the components of the velocity and force, and δ_{ij} is the identity tensor. Note that there is a negative sign in the above equation because f_{j0} has been defined as the force exerted by the fluid on the monomers. In a suspension of particles, there is screening of the hydrodynamic velocity disturbance due to the presence of surrounding particles, and the Oseen tensor for the screened hydrodynamic interactions reads (Doi and Edwards,¹⁰ Chapter 5) as

$$v_{i1}(0) = -\frac{1}{8\pi\eta r} \left(\delta_{ij} + \frac{r_i r_j}{r^2} \right) \exp(-r/\xi_H) f_{j0}(\mathbf{r}) \quad (2.8)$$

where ξ_H , the hydrodynamic screening length, is $2/(\pi c b^2)$, and c is the concentration of the monomers. The total velocity disturbance is calculated by integrating the product of the velocity disturbance and the monomer concentration over all space.

In an unstrained brush, the symmetry of the distribution of the monomers ensures that there is no net velocity in the y direction, but when the brush is deformed, the force exerted by the monomers does tend to cause a net flow in the y direction due to the asymmetry of the pair distribution function. However, this flow is not permitted in a brush of infinite extent, since it would require a flow in the y direction at the grafting surface. This can be easily seen by considering the mass conservation equation for the fluid flow:

$$\partial v_x / \partial x + \partial v_y / \partial y = 0 \quad (2.9)$$

For a steady unidirectional flow the mean velocity v_x is independent of the x direction, and from the mass conservation condition we can conclude that the v_y is independent of y . The velocity v_y at the grafting surface is zero because there is no solvent flow through this surface, and from the above considerations we can conclude that the mean velocity v_y is zero throughout the brush. In practical situations the flow is not strictly one-dimensional, since the brush has a finite extent. In this case, the first term in the above equation scales as v_{x0}/X , where X is the extent of the brush in the x direction. This indicates that v_y is, at most, $O(v_{x0}L/X)$. In the limit $X \gg L$, this is equivalent to the condition that the leading order velocity in the y direction is zero.

The velocity disturbance at the origin, $v_{y1}(0)$ due to the force exerted on the fluid by a monomer at \mathbf{r} , is given by (2.8):

$$v_{y1}(0) = \frac{-1}{8\pi\eta r} \left(f_x \left(\frac{r_x r_y}{r^2} \right) + f_y \left(1 + \frac{r_y^2}{r^2} \right) \right) \exp(-r/\xi_H) \quad (2.10)$$

Here f_x and f_y are the forces on the monomers at \mathbf{r} in the x and y directions, respectively. The total velocity disturbance is calculated by adding the effects of the monomers distributed along their classical trajectories. The averaging procedure is described in detail in the appendix; here we briefly describe the approximations involved and state the results. Consider the monomers located along inclined classical trajectories as shown in Figure 1. Here, we have chosen the origin to be midway between two classical trajectories, but the average velocity is insensitive to different choices of the position of the

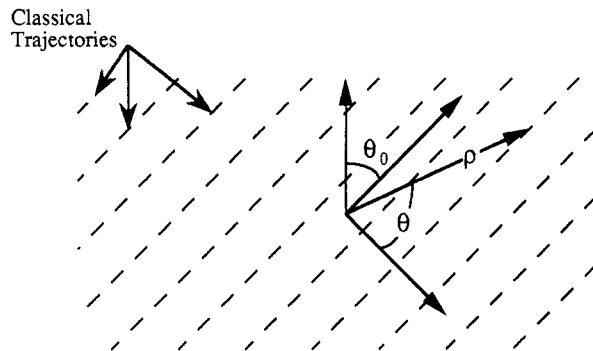


Figure 1. Schematic of the deformed classical trajectories in a polymer subjected to shear flow and the coordinate systems used for calculating the hydrodynamic interactions.

origin. The number of monomers required to traverse a unit distance in the y direction, $(\partial n)/(\partial y_n)$, is n_y , and the separation of the classical trajectories in the x direction is d . The angle of inclination of the trajectories from the vertical is θ_0 .

In the averaging procedure, it is assumed that the distribution of monomers is uniform along the classical trajectories and that these trajectories are infinite in extent. We also assume that the fluid velocity is uniform in the region under consideration and that the angle of inclination of the classical trajectories, θ_0 , is a constant. The velocity disturbance at the origin is caused by monomers located within a distance of $O(\xi_H)$, and therefore the relative error incurred due to the neglect of the variation in the density and velocity is $O(\xi_H/L)^2$. Note that the $O(\xi_H/L)$ correction vanishes due to the symmetry of the system. In the semidilute regime, the correction is small since ξ_H/L is $O(d^2/Nb^2)$, the ratio of the grafting distance, and the equilibrium radius of gyration of the brush. For the brush used by Klein et al.,⁷ $(\xi_H/L)^2$ is $O(0.1)$ and may cause an error of the same order of magnitude. The assumption that the brush is infinite in extent would overestimate the perturbation to the velocity field near the top and the bottom of the brush. However, in this analysis we calculate the ratio of the forces in the horizontal and vertical directions, and this ratio should be less sensitive to the above approximations than the actual velocity disturbances themselves. Finally, we note that the averaging procedure derived in the appendix can easily be modified to account for variations in the monomer density and fluid velocity, but this would require us to carry out the calculations numerically.

We adopt a cylindrical coordinate system (ρ, θ, z) as shown in Figure 1. The expression for the velocity disturbance is integrated over the ρ and θ coordinates to give an expression that depends only on the angle θ_0 and the forces on the monomers f_x and f_y . The relation between f_x and f_y is calculated by setting this expression equal to zero, thereby satisfying the condition $v_{y1} = 0$. The ratio f_y/f_x is shown in Figure 2 for various values of θ_0 , the angle of inclination of the classical trajectory. This ratio has a maximum value of about 0.13 and decreases to zero at $\theta_0 = 0$ and $\theta_0 = \pi/2$.

From the above calculations, we would expect the force f_y to have the following scaling forms in the limits of small, intermediate, and large velocity:

1. In the limit of small θ_0 , the ratio f_y/f_x is $\theta_0/5$, which is $O(2\pi\eta v_{x0} d^2 / 5k_B T)$. The force exerted by the fluid, f_x , which is given by (2.3), is $6\pi\eta d v_{x0}$, and therefore f_y is $12\pi^2 \eta^2 v_{x0}^2 d^3 / 5k_B T$, and the increase in the thickness of the brush is proportional to v_{x0}^2 in this regime.

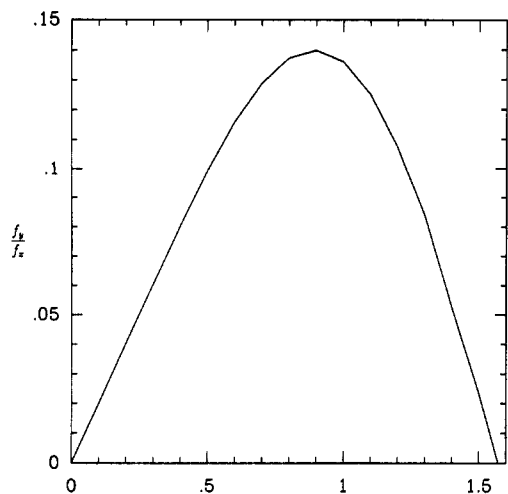


Figure 2. Ratio of the forces, f_y/f_x , as a function of the angle of inclination of the classical trajectory, θ_0 .

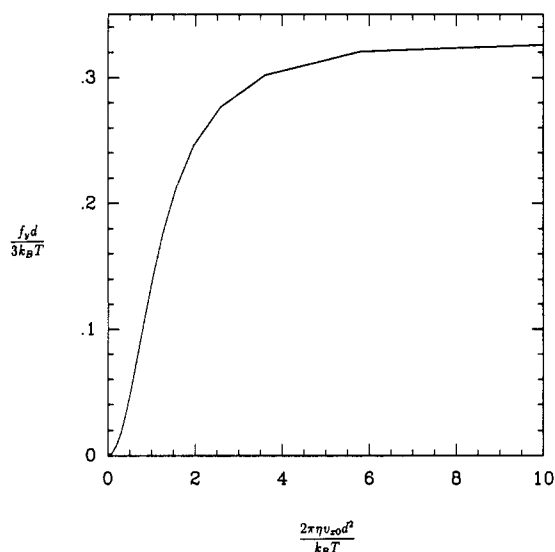


Figure 3. Dimensionless expansion of a blob, $f_y d / 3k_B T$, as a function of the dimensionless velocity, $2\pi\eta v_{x0} d^2 / k_B T$.

2. As the fluid velocity increases, the ratio f_y/f_x reaches a maximum, and in this regime we would expect the brush expansion to be proportional to v_{x0} .

3. In the limit of large v_{x0} , the ratio f_y/f_x is $(1/3)(\pi/2 - \theta_0)$. In this limit, the angle of inclination θ_0 is $\pi/2 - k_B T / 2\pi\eta v_{x0} d^2$. From these relations, it can be easily verified that the force on a blob, f_y , reaches a constant value of $k_B T/d$, and the expansion of the blobs reaches a maximum of 33%.

Figure 3 shows $f_y d / 3k_B T$, which is proportional to the expansion of a blob due to the force f_y , as a function of $2\pi\eta v_{x0} d^2 / k_B T$.

The expansion of the concentration blob due to the fluid flow can now be estimated for the brush parameters given in Table I. For an angle of inclination of $O(1)$, the maximum ratio f_y/f_x is about 0.13. The force, f_x , exerted due to the fluid flow on one concentration blob in the polymer scales as $6\pi\eta v_{x0} d$, and therefore the force f_y is $O(2.5\eta v_{x0} d)$. The expansion of the blob due to the force f_y is $f_y d^2 / 3k_B T$, which is about $0.05d$ for the parameters listed in Table I. Thus, this theory predicts a maximum brush expansion of about 5%, which is smaller than the expansion of up to 20% reported by Klein et al.⁷ It should be cautioned that this analysis can provide only order of

magnitude estimates of the brush expansion, and not numerically accurate values, because we have made a number of simplifying assumptions. However, we would not expect our analysis to change the order of magnitude of the results, since the important intermediate step is the calculation of the ratio of the forces on a monomer in the x and y directions, and this ratio will not be as sensitive to our assumptions as the actual values of the forces themselves.

III. Conclusions

In this paper, we have studied the effect of hydrodynamic interactions on the dynamics of a polymer brush in shear flow. This analysis was motivated by experiments conducted by Klein et al.,⁷ who used a surface force apparatus to measure the thickness of a brush under shear flow. They reported that the brush thickness could increase by up to 20% due to the flow.

The important length and time scales in the system were determined by a scaling analysis using realistic brush parameters. The response time of the polymer is about 0.27×10^{-5} s, and we can use a static analysis for the flow and strain fields if the frequency of oscillation is small compared to this. The frequency used by Klein et al.⁷ was $O(10^2 \text{ s}^{-1})$, and a static analysis is justified for this case. The important length scales in the brush are the height, L , the grafting distance, d , and the hydrodynamic screening length, ξ_H . In a strongly stretched brush, the screening length is $O(d/b)^{1/3}$ larger than the grafting distance d but $O(d/R_G)^2$ smaller than the height L . Our analysis of the hydrodynamic interactions is carried out in the limit $d \ll \xi_H \ll L$, which is valid for a strongly stretched brush. This may not be strictly valid for the brushes of the type used by Klein et al.,⁷ because d is smaller than L only by a factor of about 10, and this may not leave adequate room for an intermediate scale. However, the results are in good qualitative agreement with the experiments and predict a swelling of the correct magnitude.

The expansion of the brush is calculated using a perturbation analysis. The change in the conformation of the equilibrium brush due to the fluid flow is first calculated, and this is substituted into the equations for the hydrodynamic interactions to calculate the swelling of the brush. In a highly stretched brush at equilibrium, the positions of the monomers fluctuate by a distance of $O(d)$ about the classical paths perpendicular to the grafting surface. If a shear flow is applied to the brush, the classical paths deviate from their equilibrium configurations due to the frictional force exerted by the fluid. The hydrodynamic interactions in this strained brush tend to cause a net fluid velocity in the direction perpendicular to the grafting surface. The reason for this can be visualized as follows. Consider a particle at the origin surrounded by four particles distributed symmetrically in the four quadrants as shown in Figure 4. If there is a fluid flow in the $+x$ direction, the hydrodynamic velocity disturbance due to the particles in the first and third quadrants is directed in the $-y$ direction, while the disturbance due to the particles in the second and fourth quadrants is in the $+y$ direction. When the brush deforms, the particles in the second and fourth quadrants shift closer to the origin, while those in the first and third quadrants shift further away, as shown by the broken lines in Figure 4. Since the magnitude of the velocity disturbance due to hydrodynamic interactions is inversely proportional to the distance between the particles, the deformation increases the effect of the particles in the second and fourth quadrants and decreases the effect of the particles in the first and third

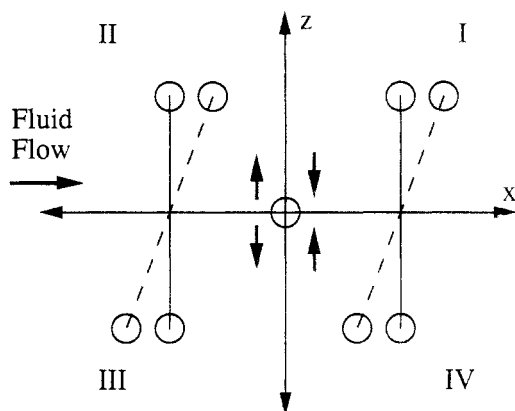


Figure 4. Schematic of the physical mechanism causing the brush expansion. The fluid velocity in the y direction at the origin due to the presence of particles in the four quadrants is shown by the bold arrows near the origin. The deformation of the brush brings the particles in the second and fourth quadrants closer to the origin and moves the particles in the first and third quadrants further away and thereby tends to cause a net upward flow.

quadrants, thus tending to cause a net upward flow. However, a flow in the y direction is not permitted due to the mass conservation condition, and to suppress this flow, a pressure gradient is set up in the y direction. This pressure gradient exerts a net force on the polymers perpendicular to the grafting surface, which results in an increase in the thickness. We derived the ratio of the forces f_y/f_x required to ensure that the velocity perpendicular to the grafting surface is zero. In the analysis we assumed that the fluid velocity and polymer strain are constant over distances of $O(\xi_H)$ and that the brush is infinite in extent. However, the ratio of the forces in the two directions will not be as sensitive to these assumptions as the actual values of the forces or velocity disturbances themselves.

The increase in the brush thickness is proportional to the square of the fluid velocity at the surface for small deviations from the equilibrium configuration but increases as a linear function of the fluid velocity for larger deviations. In the limit of large velocities, we would expect the brush expansion to increase to a maximum of 33%. However, at such large expansions, the second-order terms in the perturbation expansion would become important and the analysis carried out in this paper may not be valid. Interestingly, Barrat⁸ also predicted that there is a maximum value of about 25% for the brush expansion using a completely different mechanism. He approximated the shear flow by a constant force acting at the surface of the brush and showed that this force reduces the osmotic compressibility of the brush and causes it to swell. One method to distinguish between these two mechanisms is by applying a force at the surface of the brush by a nonhydrodynamic method, such as a magnetic field. If the swelling observed in this experiment is comparable to that observed in the shear flow experiments, it implies that the expansion is indeed due to a decrease in the osmotic pressure and not due to hydrodynamic interactions. Barrat's theory also predicts that the extension of the chains in the direction of flow is large compared to the increase in the thickness of the brush. For example, his calculation indicates that, to obtain an expansion in the brush thickness of 150 Å, it is necessary to stretch the chains in the direction of flow by 2400 Å. Experimental observation of the local strain in the brush could also help differentiate between the two mechanisms.

We estimated the increase in the thickness for the brush used by Klein et al.⁷ to be about 5%, which is smaller than the value of about 20% reported by them. The discrepancy may be due to the approximations that have been made, which prevent us from getting numerically accurate values. In particular, we have used a perturbation method to calculate the brush expansion, and this may not be valid for expansions as large as 20%. There may also be uncertainties in the values of some experimental parameters such as the grafting distance, d . However, our theory agrees qualitatively with experiments, and the observed 20% increase in thickness is well within the maximum possible increase of 33% predicted by the theory.

Acknowledgment is made to the donors of the Petroleum Research Fund, administered by the American Chemical Society, for support of this research. The author had instructive discussions with Prof. G. H. Fredrickson and Prof. P. Pincus.

Appendix A

In this appendix, we estimate the force exerted on a monomer due to hydrodynamic interactions with the surrounding monomers in the brush. For the purposes of this calculation, the number density and the fluid velocity are assumed to be constant within a sphere of radius ξ_H surrounding the monomer. The configuration of the monomers and the coordinate systems are shown in Figure 1. The test monomer is located at the origin, and the surrounding monomers are distributed along the classical trajectories of the polymers which intersect the x - z plane at $((i + 1/2)d, 0, (j + 1/2)d)$, where i and j are integers which will be used to label the trajectories. The number of monomers per unit distance in the y direction along a trajectory is n_y , and the trajectories are inclined at an angle θ_0 relative to the y direction due to the fluid flow. It is convenient to analyze the effect of pairs of trajectories $(\pm i, j)$ distributed symmetrically about the origin. We define a cylindrical coordinate system (ρ, θ, z) , as shown in Figure 1. Along the trajectory, the radial coordinate, ρ , is related to the polar angle, θ , as follows:

$$\rho = \frac{(i + 1/2)d \cos(\theta_0)}{|\cos(\theta)|} \quad (\text{A1})$$

We define a linear number density of monomers, n_θ , such that $n_\theta \rho d\theta$ is the number of monomers in the differential angle $d\theta$ about θ . It can easily be verified that n_θ is related to n_y as follows:

$$n_\theta = n_y |\cos(\theta - \theta_0)| \quad (\text{A2})$$

The velocity disturbance at the origin, v_{y1} , due to the force exerted on the fluid by another monomer at (ρ, θ, z) , can be calculated from (2.10):

$$v_{y1} = - \left(\frac{1}{8\pi\eta(\rho^2 + z^2)^{1/2}} \right) \times \exp\left(-\frac{(\rho^2 + z^2)^{1/2}}{\xi_H}\right) (f_x a_x + f_y a_y) \quad (\text{A3})$$

where a_x is $\cos(\theta - \theta_0) \sin(\theta - \theta_0)$, and a_y is $1 + \sin^2(\theta - \theta_0)$. The total force is calculated by integrating the above expression along the trajectory (i, j) and adding the contributions for trajectories having values of i from 1 to ∞ and j from $-\infty$ to ∞ .

$$V_{y1} = \sum_{i=1}^{\infty} \sum_{j=-\infty}^{\infty} \int_0^{2\pi} v_{y1} n_\theta \rho d\theta \quad (\text{A4})$$

The summations over the indices i and j can be transformed

into integrals in the limit $d \ll \xi_H$, and evaluated analytically, to give the following expression:

$$V_{y1} = -\left(\frac{\xi_H}{d}\right)^2 \left(\frac{n_y}{4\pi\eta}\right) \int_0^{2\pi} d\theta \frac{|\cos(\theta)| |\cos(\theta - \theta_0)|}{\cos(\theta_0)} (f_x a_x + f_y a_y) \quad (\text{A5})$$

The ratio f_y/f_x is calculated by setting the right side of the above expression equal to zero. This ratio is shown as a function of θ_0 in Figure 2.

References and Notes

- (1) Halperin, A.; Tirrell, M.; Lodge, T. P. *Adv. Polym. Sci.* **1991**, *100*, 200.
- (2) Alexander, S. J. *J. Phys.* **1977**, *38*, 983.
- (3) de Gennes, P.-G. *Macromolecules* **1980**, *13*, 1069.
- (4) Milner, S. T.; Witten, T. A.; Cates, M. E. *Macromolecules* **1988**, *21*, 2610.
- (5) Tounton, H. J.; Toprakcioglu, C.; Fetters, L. J.; Klein, J. *Macromolecules* **1990**, *23*, 571.
- (6) Rabin, Y.; Alexander, S. *Europhys. Lett.* **1990**, *13*, 49.
- (7) Klein, J.; Perahia, D.; Warburg, S. *Nature* **1991**, *143*, 352.
- (8) Barrat, J.-L. *Macromolecules* **1992**, *25*, 832.
- (9) Milner, S. *Macromolecules* **1991**, *24*, 3704.
- (10) Doi, M.; Edwards, S. F. *The Theory of Polymer Dynamics*; Oxford Science Publications: Oxford, U.K., 1989.
- (11) Brinkman, H. C. *Appl. Sci. Res.* **1947**, *61*, 3626.